JOURNAL OF SOLID STATE CHEMISTRY 13, 24–31 (1975)

Optical and Electronic Properties of some New Rare Earth-Doped Lead Sodium Apatites

L. H. BRIXNER AND P. E. BIERSTEDT

Central Research Department, E. I. du Pont de Nemours and Company, Wilmington, Delaware 19898*

Received January 28, 1974

Single crystals of the anion-deficient apatite of formula $Pb_8Na_2(PO_4)_6\varnothing_2$ as well as rare earth-doped compositions of the type $Ln_xPb_{8-x}Na_2(PO_4)_6\varnothing_{2-x/2}O_{x/2}$ with Ln = Ce, Pr, Nd, Sm, Eu, Gd, Tb, Dy, Ho, and Er have been grown by the Czochralski technique. All crystallize in the $P6_3/m$ space group of apatite with c_h about 7.20 Å and a_h about 9.73 Å. Transmission, excitation, and fluorescence spectra were obtained on many single crystals and are discussed. Anomalous dielectric behavior indicating ionic conduction is also presented. It is further shown that the often quoted "lead orthophosphate of apatite structure, $Pb_3(PO_4)_2$" is actually not pure lead phosphate but rather a sodium stabilized apatite of the composition $Pb_{8+x}Na_{2-x}(PO_4)_6\varnothing_{2-x/2}O_{x/2}$.

Introduction

Lead orthophosphate, $Pb_3(PO_4)_2$, with the apatite structure has been reported in the literature as early as 1928, when Zambonini (*1*) recognized the similarity of its X-ray pattern with the mineral pyromorphite, $Pb_{10}(PO_4)_6Cl_2$ which is a true apatite. Roehl (*2*) and Klement (*3*) later described the same modification and Paetsch and Dietzel (*4*) were the first to state that this composition might actually be a hydroxy apatite and not a pure lead phosphate. In 1957 Merker and Wondratschek (*5*) reported the existence of alkali lead apatites of the formula $Pb_8M_2(PO_4)_6\varnothing_2$, and later (*6*) they reported on the alkali-free apatite $Pb_{10}(PO_4)_6O$. From this information, we assumed that solid solutions between these two end members of the type $Pb_{8+x}M_{2-x}(PO_4)_6\varnothing_{2-x/2}O_{x/2}$ should exist over the complete range of x from 0 to 2.

In the present paper we will show that sodium levels of less than 1 % will stabilize the apatite structure. Also, it will be shown that any lead phosphate preparation involving precipitation from alkali salt solutions will produce this form. It is interesting to note that as late as 1973 Osterheld and Hawthorne (*7*) stated that they "could not find" $Na_2Pb_8(PO_4)_6$ ($x = 0$) during their studies of the $Na_3PO_4/Pb_3(PO_4)_2$ system. This is surprising since the compounds are stable and melt congruently and it can only be explained if one assumes that their poorly characterized $Pb_3(PO_4)_2$ already *was* of the apatite structure.

Rare earth substitution in the apatite $Ca_{5-3x/2}Nd_x(PO_4)_3F$ has been studied by Mazelski et al. (*8*), who found exceptionally low threshold values for Nd lasers based on this compound. Assuming that it is the $P6_3/m$ crystal field environment for Nd which brought about this composition's superior laser properties, we considered the Nd-doped lead sodium apatite as a laser composition. Although it is much easier to grow than the fluoroapatite, the lower hardness of the lead sodium apatite will be a disadvantage in its potential laser application.

Also, since the apatite structure contains channels or tunnels parallel to the c-axis, the possibility of anionic conduction along these channels was considered. To investigate this, dielectric methods were used to obtain the

---

*Contribution No. 2117.

Printed in Great Britain

relaxation and dispersion information which would arise from the mobility of oxygen along these channels.

Experimental

During a study of the crystal growth behavior of α and β-$Pb_3(PO_4)_2$ (*9*), a variety of procedures was used to prepare feed material. One of these procedures involved the precipitation of lead phosphate by combining solutions of Na_3PO_4 and $Pb(NO_3)_2$ according to:

$$3Pb(NO_3)_2 + 2Na_3(PO_4) \rightarrow Pb_3(PO_4)_2 + 6NaNO_3$$

The product was filtered, dried, and fired at 800°C. This feed material was then used for the single crystal growth, which was carried out in pure platinum containers. A 20 KVA "Ecco" 450 kHz rf unit served as a power supply. Rotation rates were generally kept between 40 and 60 rpm at growing speeds of .25–.5 in./hr. Growth was first initiated on a Pt wire but subsequent runs were carried out on seeds oriented and cut in specific crystallographic directions. The rare earth containing compounds were prepared by solid state reactions between Na_2CO_3, $PbCO_3$, $NH_4H_2PO_4$ and the appropriate Ln_2O_3 compound.

X-Ray Studies

Single crystal photographs were taken with a precession camera using Mo radiation. X-ray powder patterns were obtained with a Guinier–Hägg camera at 25°C with CuK_α radiation and an internal standard of KCl ($a = 6.2931$ Å). Refined cell dimensions were obtained by a least-squares treatment of the Guinier data. The fluorescence, excitation, and absorption spectra were all obtained with a Cary Model 17 spectrometer.

Electrical Studies

A study of the directional dependence of the dielectric properties was made on single crystal specimens. The crystals were X-ray oriented so that measurements could be taken with the electric field either parallel or perpendicular to the c-axis. Air dry silver paint (Du Pont No. 4922) was used to form the electrodes and values of the dielectric constant (K') were derived from the capacitance as measured on an automatic capacitance bridge (HP Model 4270A). This bridge also measured the equivalent parallel conductance (G). These measurements, made at frequencies of 10^3, 10^4, 10^5, and 10^6 Hz, covered the temperature range −196–600°C. The temperature was monitored with a chromel–alumel thermocouple, whose output provided the X voltage for a Mosley 2D–2A X–Y recorder. The capacitance output of the bridge, converted from digital-to-analog information, provided the Y voltage. Thus, the recorder trace provided a continuous measurement of the sample capacitance vs temperature. The conductance output of the bridge applied in the same manner to a second X–Y recorder, yielded a continuous measurement of G vs temperature.

Results and Discussion

Structure

When we refined the cell parameters of the very first crystal grown, we believed we had the "hexagonal $Pb_3(PO_4)_2$" form reported by Wyckoff (*10*). The comparison is shown in Table I. The lattice parameters of $a = 9.7$ Å and $c = 7.12$ Å, also compared well with our values of $a = 9.7821$ Å and $c = 7.3029$ Å. However, a space group determination indicated $P6_3/m$ symmetry which is that of the apatite structure. A hydroxyl apatite [as suggested by Paetsch and Dietzel (*4*)] was unlikely to survive the melt temperature of nearly 1000°C and no chloride was present in the starting materials to produce a chloro apatite. We therefore rejected the possibility of our product being either a hydroxyl or chloroapatite, and looked for another formulation of an apatite, based on the constituent components Na, Pb, P, and O. Such a compound has been reported by Merker and Wondratschek (*5*) in the form of $Na_2Pb_8(PO_4)_6\varnothing_2$ with two complete vacancies in the normal X_2 sites. In the present situation we are not dealing with this pure compound, but rather with a sodium-deficient version of the type $Pb_{8+x}Na_{2-x}(PO_4)_6O_{x/2}\varnothing_{2-x/2}$ with an x value of approximately one.

TABLE I

Comparison of Single Crystal Data with Literature Values on Hexagonal $Pb_3(PO_4)_2$

Literature (9)			This Work		
Intensity	d	hkl	Intensity	$d_{(obsd)}$	$d_{(calcd)}$
	—	101	20	5.4841	5.4764
	—	110	25	4.8644	4.8679
m	4.18	200	80	4.2141	4.2157
ms	3.99	111	85	4.0325	4.0331
mw	3.57	002	65	3.6005	3.6013
m	3.29	102	85	3.3115	3.3118
m	3.17	210	90	3.1872	3.1867
	—	211	100	2.9141	2.9142
vs	2.88	112	95	2.8958	2.8951
s	2.79	300	90	2.8099	2.8104
	—	301	10	2.6173	2.6182
	—	212	15	2.3867	2.3865
	—	310	25	2.3386	2.3384
	—	221	5	2.3032	2.3058
	—	103			2.3090
m	2.143	113	75	2.1534	2.1532
	—	400	50	2.1079	2.1078
w	2.099	203	10	2.0861	2.0862
ms	2.012	222	75	2.0167	2.0165

This conclusion is based on an extrapolation of lattice parameters, as given by Engel (*11*), for both the pure oxyapatite $Pb_{10}(PO_4)_6O\varnothing$ ($x = 2$) and the pure sodium compound $Na_2Pb_8(PO_4)_6\varnothing_2$ ($x = 0$). This composition, $Pb_9Na(PO_4)_6O_{.5}\varnothing_{1.5}$, would require the presence of .93% Na, and semiquantitative spectroscopic examination of the crystals indicated ~1% Na. Wet chemical analysis gave 75.1% Pb and 7.5% P, both in excellent agreement with the calculated amounts of 75.63% Pb and 7.54% P.

The crystal grown on a Pt wire developed in almost a perfect *c*-axis orientation exhibiting six distinct growth lines running parallel to the boule axis, indicating three-fold symmetry. New *c*-oriented seeds were cut from this boule and all subsequent crystals were grown along the *c*-axis.

As the next step we attempted to grow pure $Pb_8Na_2(PO_4)_6\varnothing_2$ by using stoichiometrically prepared feed. The crystal did not have this exact formula, due to a segregation coefficient for Na less than one. This composition has the formula $Pb_{8.5}Na_{1.5}(PO_4)_6O_{.25}\varnothing_{1.75}$, and its chemical analysis and refined parameters are summarized in Table II. The DTA data were obtained on a Du Pont 900 thermal analyzer.

Optical Properties

Pure $Pb_8Na_2(PO_4)_6\varnothing_2$ does not fluoresce under either 3660 or 2537 Å excitation. But since apatite structures (*8*, *12*) have been extensively used as hosts for fluorescing ions, we undertook a study of the optical properties of some of the rare earths-doped crystals. The general composition used as starting material for crystal growth was $Pb_{7.75}Ln_{.25}Na_2(PO_4)_6$-$O_{.125}\varnothing_{1.875}$, where Ln stands for the rare earths. As we showed earlier, due to segregation the true sodium concentration in the crystal is less than two moles per molecule, and therefore these are only nominal compositions. Despite the low concentrations of rare earths present, the lanthanide contraction can clearly be observed in the parameters presented in Table III.

A typical crystal of the Nd compound is shown in Fig. 1. Figures 2–5 show the fluorescent emission characteristics of the Ln ions emitting in the visible: Sm (orange), Eu (red), Tb (green), and Dy (yellow). The excitation spectra are shown in Figs. 6–9. In the case of Tb, an assignment of transitions was made based on the established energy level diagram of this ion (*13*). Figure 10 shows the ir emission of Nd at room temperature. The dominant

TABLE II

Composition and Parameters of $Pb_{8.5}Na_{1.5}(PO_4)_6O_{.25}\varnothing_{1.75}$ Single Crystals

				% Pb		% Na		% P		% O	
a (Å)	c (Å)	V(Å^3)	°C mp (DTA)	Found	Calcd	Found	Calcd	Found	Calcd	Found	Calcd
9.7358	7.2026	591.24	987	73.9	74.33	1.55	1.45	8.1	7.84	16.6	16.38

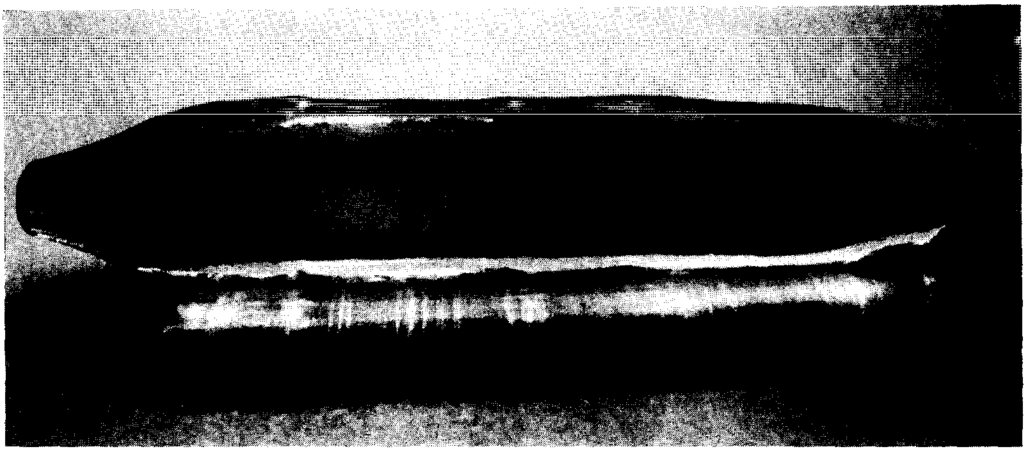

FIG. 1. Single crystal of czochralski grown $Pb_{7.75}Nd_{.25}Na_2(PO_4)_6O_{.125}$.

TABLE III

LATTICE CONSTANTS[a] OF CZOCHRALSKI GROWN RARE-EARTH DOPED COMPOUNDS

Ln of Composition $Pb_{7.75}Ln_{.25}$-$Na_2(PO_4)_6O_{.125}$	a (Å)	c (Å)	Color
Ce	9.7407	7.2004	Yellow
Pr	9.7397	7.2006	Green
Nd	9.7368	7.1987	Blue
Sm	9.7346	7.1966	Pale orange
Eu	9.7299	7.1944	Colorless
Gd	9.7285	7.1932	Colorless
Tb	9.7261	7.1917	Colorless
Dy	9.7254	7.1896	Pale yellow
Ho	9.7233	7.1890	Pale brown
Er	9.7201	7.1886	Pink

[a] The cell dimensions are accurate to ±0.0005 Å for a and ±0.0004 for c.

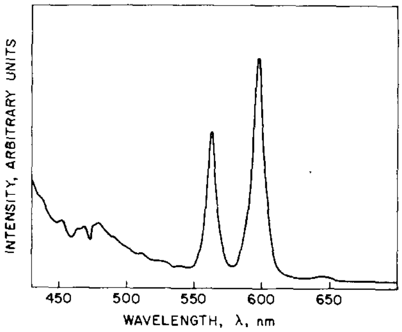

FIG. 2. Fluorescent emission spectrum of $Pb_{7.75}$-$Sm_{.25}Na_2(PO_4)_6O_{.125}$.

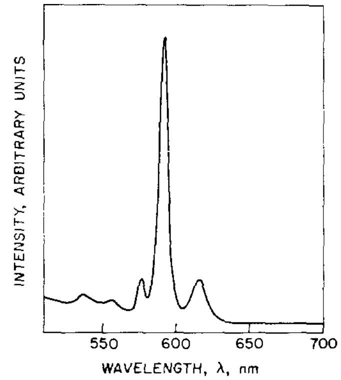

FIG. 3. Fluorescent emission spectrum of $Pb_{7.75}$-$Eu_{.25}Na_2(PO_4)_6O_{.125}$.

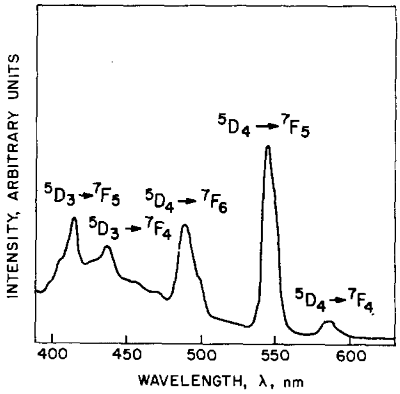

FIG. 4. Fluorescent emission spectrum of $Pb_{7.75}$-$Tb_{.25}Na_2(PO_4)_6O_{.125}$.

line is at 1.0547 μm with a half width of about 50 Å. Two minor peaks are observed at 1.0645 and 1.0680 μm, each with 5 Å half width. Figure 11 shows a high resolution absorption spectrum of the Nd compound. The important $4F_{3/2}$ absorption level (the closest to the 1.06 μm emission) is indicated. With an injection

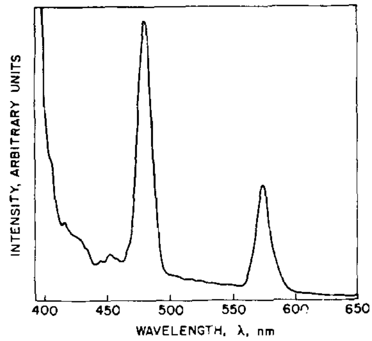

FIG. 5. Fluorescent emission spectrum of $Pb_{7.75}$-$Dy_{.25}Na_2(PO)_4)_6O_{.125}$.

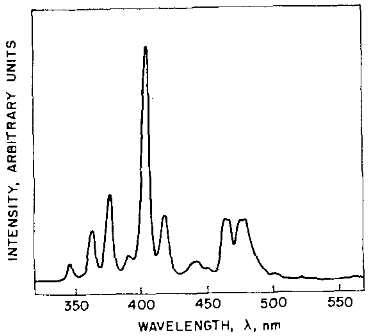

FIG. 6. Excitation spectrum of $Pb_{7.75}Sm_{.25}Na_2$-$(PO_4)_6O_{.125}$.

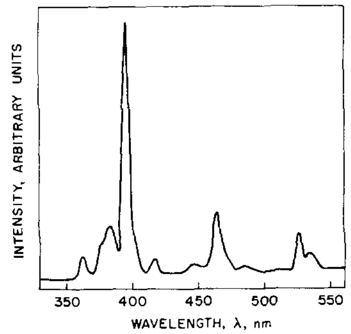

FIG. 7. Excitation spectrum of $Pb_{7.75}Eu_{.25}Na_2$-$(PO_4)_6O_{.125}$.

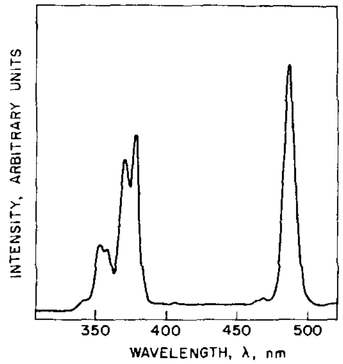

FIG. 8. Excitation spectrum of $Pb_{7.75}Tb_{.25}Na_2$-$(PO_4)_6O_{.125}$.

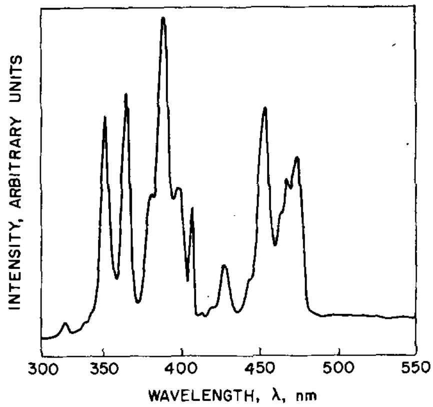

FIG. 9. Excitation spectrum of $Pb_{7.75}Dy_{.25}Na_2$-$(PO_4)_6O_{.125}$.

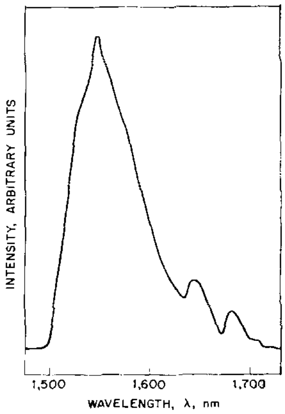

FIG. 10. Fluorescent emission spectrum of $Pb_{7.75}$-$Nd_{.25}Na_2(PO_4)_6O_{.125}$.

laser emitting in this region, there is the potential for direct pumping. Unfortunately, the absorption is only very slightly different from that of Nd in other hosts (*12*). The absorption spectra of the other colored ions, absorbing in the visible (Pr, Sm, Ho, and Er), are shown in Figs. 12–15. A far ir spectrum for the Gd compound is shown in Fig. 16. This ir spectrum must be due to the host since it was essentially unchanged for all compositions examined. The 5 μm absorption is most likely an overtone of the 10 μm vibrational frequency commonly observed for phosphates.

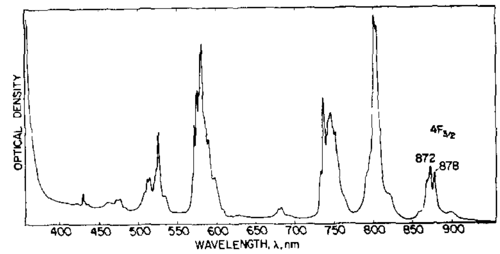

FIG. 11. Absorption spectrum of Pb$_{7.75}$Nd$_{.25}$Na$_2$(PO$_4$)$_6$O$_{.125}$.

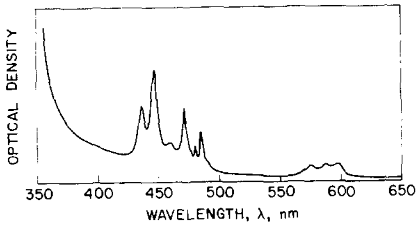

FIG. 12. Absorption spectrum of Pb$_{7.75}$Pr$_{.25}$Na$_2$(PO$_4$)$_6$O$_{.125}$.

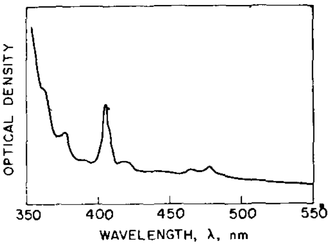

FIG. 13. Absorption spectrum of Pb$_{7.75}$Sm$_{.25}$Na$_2$(PO$_4$)$_6$O$_{.125}$.

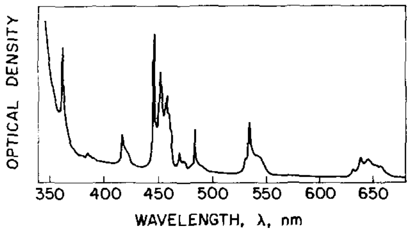

FIG. 14. Absorption spectrum of Pb$_{7.75}$Ho$_{.25}$Na$_2$(PO$_4$)$_6$O$_{.125}$.

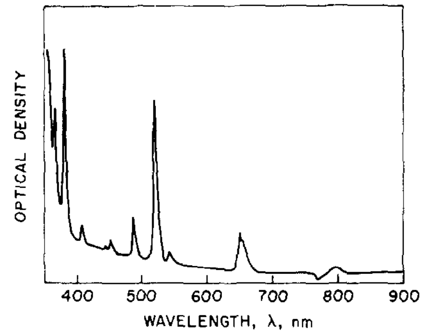

FIG. 15. Absorption spectrum of Pb$_{7.75}$Er$_{.25}$Na$_2$(PO$_4$)$_6$O$_{.125}$.

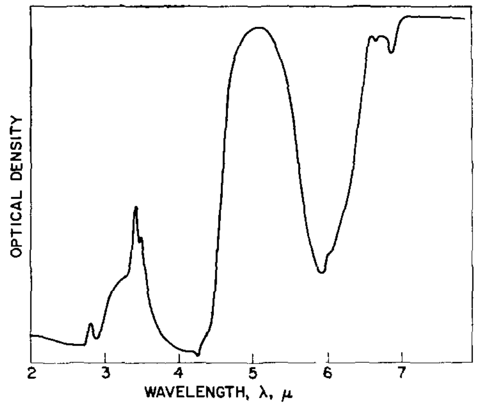

FIG. 16. Infrared absorption spectrum of Pb$_{7.75}$Gd$_{.25}$Na$_2$(PO$_4$)$_6$O$_{.125}$.

Dielectric Behavior

The observation of frequency-dependent capacitance and conductance in ionic conductors is well known. Peaks in the loss factor (either vs frequency at constant temperature, or vs temperature at constant frequency) have been used (*14*) to get activation energies and information on relaxation times; and such behavior was observed in the compound studied here.

Dielectric measurements were made along the *c*-axis on a crystal of Pb$_{8.5}$Na$_{1.5}$(PO$_4$)$_6$O$_{.25}$$\varnothing_{1.75}$. Low temperature studies revealed a peak in the dielectric loss (K'') and the temperature of the peak increased as the measuring frequency increased. From these dielectric loss data, the activation energy of the conduction mechanism is obtained. A plot of the log of the frequency (f) vs $1/T_{\max}$, where $T_{\max}$ is the temperature at which the loss peak occurs, yields a linear plot having the equation $f = f_0 e^{-E_a/kT}$. From this plot an activation energy E_a of 0.34 eV was obtained. The activation energy was also obtained from a plot of log σT vs $10^3/T$, where σ is the ac conductivity and this value is 0.35 eV, in excellent agreement with the above value.

In addition, we observed that the dielectric constant (K') measured along the c-axis has a significant frequency dependence at high temperature. Similar measurements perpendicular to the c-axis revealed no unusual properties. This behavior, shown in Figs. 17 and 18, is consistent with the fact that in the apatite structure the X_2 sites are arranged in channels along the c (or 6_3) axis. It is therefore assumed that in this sodium-deficient structure, the dielectric data reflect oxygen mobility in these channels. A recent review by Whittingham and Huggins on ionic transport in solids with channel or tunnel structures (*15*) does not report any anionic conductors. We therefore believe that anion conduction in channels is a unique property, and is probably much less common than cationic conduction transport in crystallographic tunnels. NMR line-narrowing experiments for Na were negative further supporting the anionic conduction.

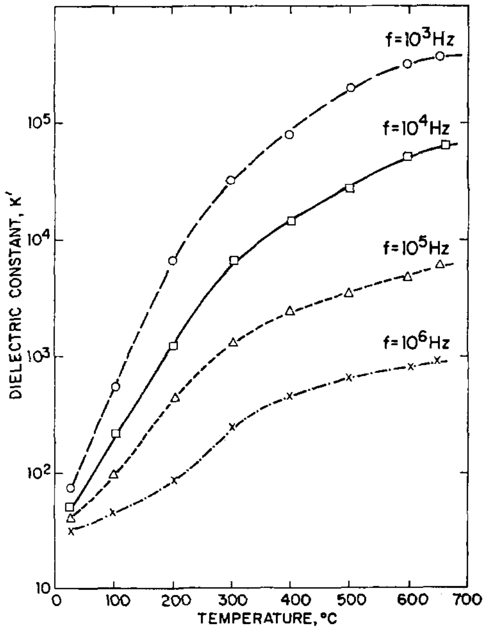

FIG. 17. Dielectric constant of $Pb_{8.5}Na_{1.5}(PO_4)_6$-$O_{.25}$ measured along c-axis.

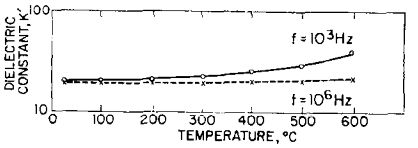

FIG. 18. Dielectric constant of $Pb_{8.5}Na_{1.5}(PO_4)_6$-$O_{.25}$ measured perpendicular to c-axis.

Chemical Modification

If one attempts to get total occupancy of the X_2 sites by O_2, the Na has to be completely replaced with a trivalent ion. Such an attempt was made with the compound $Pb_8Bi_2(PO_4)_6$-O_2. However, this compound no longer crystallized in the apatite structure but rather in one with orthorhombic symmetry having possible space groups of *Pnma* or *Pn*2_1. The latter is ruled out based on the absence of a signal from a second harmonic generation test carried out in equipment similar to that described by Perry et al. (*16*). The parameters found for $Pb_8Bi_2(PO_4)_6O_2$ [which might actually constitute a "bismutyl" compound with the BiO^{+1} ion and be formulated Pb_4BiO-$(PO_4)_3$] were: $a = 13.313 \pm 2$ Å; $b = 10.284 \pm 1$ Å; $c = 9.219 \pm 1$ Å; $V = 1262.35$ Å^3.

Acknowledgments

It is a pleasure to thank C. M. Foris for her assistance in obtaining the X-ray data and E. Wallace for running the spectra.

References

1. F. ZAMBONINI, *Atti Accad. Naz. Lincei, Cl. Sci. Tais., Mat. Natur., Rend.* **6**, 283 (1928).
2. E. J. ROEHL, *J. Amer. Chem. Soc.* **61**, 2249 (1939).
3. R. KLEMENT, *Z. Anorg. Chem.* **237**, 161 (1938).
4. H. H. PAETSCH AND A. DIETZEL, *Glastech. Ber.* **29**, 345 (1956).
5. L. MERKER AND H. WONDRATSCHEK, *Z. Kristallogr. Kristallgeometric Kristallphys. Kristallchem.* **109**, 110 (1957).

6. L. Merker and H. Wondratschek, *Z. Anorg. Allg. Chem.* **306**, 25 (1960).
7. R. K. Osterheld and J. D. Hawthorne, *J. Solid State Chem.* **7**, 106 (1973).
8. R. Mazelski, R. C. Ohlmann, and K. Steinbruegge, *J. Electrochem. Soc.* **115**, 67 (1968).
9. L. H. Brixner, P. E. Bierstedt, W. F. Jaep, and J. R. Barkley, *Mater. Res. Bull.* **8**, 497 (1973).
10. R. W. G. Wyckoff, "Crystal Structures," Vol. 3, Wiley, p. 233. New York, 1960.
11. G. Engel, *J. Solid State Chem.* **6**, 286 (1973).
12. L. H. Brixner, *J. Electrochem. Soc.* **112**, 303 (1965).
13. G. H. Dietke, "Spectra and Energy Levels of Rare Earth Ions in Crystals," p. 8. Wiley, New York, 1968.
14. R. H. Radzilowski, Y. F. Yao, and J. T. Kummer, *J. Appl. Phys.* **40**, 4716 (1969).
15. M. S. Whittingham and R. A. Huggins, "Reactivity of Solids" (J. S. Anderson, M. W. Roberts, and F. S. Stone, Eds.), p. 125. Chapman and Hall, London, 1972.
16. S. K. Perry and T. T. Kurtz, *J. Appl. Phys.* **39**, 3798 (1968).